FILE COPY
NO. 1-W

NACA-WRL. 586

NATIONAL ADVISORY COMMITTEE FOR AERONAUTICS

WARTIME REPORT

ORIGINALLY ISSUED
November 1944 as
Memorandum Report L4K30

BENDING AND SHEAR STRESSES DEVELOPED BY THE INSTANTANEOUS ARREST OF THE ROOT OF A CANTILEVER BEAM WITH A MASS AT ITS TIP

By Elbridge Z. Stowell, Edward B. Schwartz,
John C. Houbolt, and Albert K. Schmieder

Langley Memorial Aeronautical Laboratory
Langley Field, Va.

FILE COPY
To be returned to
the files of the National
Advisory Committee
for Aeronautics
Washington D. C.

Reproduced by
NATIONAL TECHNICAL
INFORMATION SERVICE
U S Department of Commerce
Springfield VA 22151

NACA

WASHINGTON

NACA WARTIME REPORTS are reprints of papers originally issued to provide rapid distribution of advance research results to an authorized group requiring them for the war effort. They were previously held under a security status but are now unclassified. Some of these reports were not technically edited. All have been reproduced without change in order to expedite general distribution.

34

NATIONAL ADVISORY COMMITTEE FOR AERONAUTICS

MEMORANDUM REPORT

for the

Army Air Forces, Air Technical Service Command

BENDING AND SHEAR STRESSES DEVELOPED BY THE INSTANTANEOUS ARREST OF THE ROOT OF A CANTILEVER BEAM WITH A MASS AT ITS TIP

By Elbridge Z. Stowell, Edward B. Schwartz,
John C. Houbolt, and Albert K. Schmieder

SUMMARY

A theoretical and experimental investigation has been made of the behavior of a cantilever beam in transverse motion with a mass at its tip when the root is suddenly brought to rest. Equations are given for determining the stresses, the deflections, and the accelerations that arise in the beam as a result of the impact. The theoretical equations, which have been confirmed experimentally, reveal that for a beam with a given cross section and velocity at impact and for a given ratio of tip mass to beam mass, the bending stresses for a particular mode at a given percentage of the distance from root to tip are independent of the length of the beam; whereas, the shear stresses vary inversely with the length.

The addition of a mass to the tip of a cantilever beam increases appreciably the stresses produced by the first mode of vibration but changes only slightly the stresses contributed by the higher modes. The tip mass increases the maximum bending stress much less than might be expected on the basis of experience with the static action of structures. For practical engineering analysis the maximum bending stress developed in a suddenly arrested cantilever beam can be found by a simple addition of stress amplitudes in the first few modes without regard to phase relations between modes.

INTRODUCTION

When an airplane lands, the vertical component of the velocity is rapidly reduced to zero. The shock of the sudden change in motion gives rise to vibratory stresses in the airplane. As a beginning in the study of these stresses a previous report (reference 1) discussed in detail the behavior of a cantilever beam in translational motion when its root is suddenly brought to rest. In that paper equations are given for determining the stresses, the deflections, and the accelerations that arise throughout the beam as a result of the impact. The present report extends the basic problem of reference 1 to include the effect of a concentrated mass at the tip of the cantilever beam.

As in reference 1, the present paper is based on the usual engineering beam theory. In this theory the deflections are considered to be the result of bending alone, shear deflections neglected. The theory as applied to ordinary beams gives reasonably good results so long as the distance between inflection points is greater than a few times the depth of the beam. When this theory for beam action is used in vibration problems, such as that in the present paper, the results are satisfactory for those modes of vibration for which the nodes are not too close together.

This report summarizes the results of a theoretical solution given in appendix A and presents an experimental verification of these results. A numerical example for the calculation of the maximum stresses near the root of the cantilever beam is given in appendix B.

SYMBOLS

E modulus of elasticity

γ weight density of material

λ coefficient of equivalent viscous damping of material

c velocity of sound in material $\sqrt{\frac{Eg}{\gamma}}$

g acceleration of gravity

L length of beam

I moment of inertia of cross section of beam about neutral axis

A cross-sectional area of beam

ρ radius of gyration of cross section of beam $\left(\sqrt{\frac{I}{A}}\right)$

x coordinate along beam measured from root

y distance from neutral axis of beam to any fiber

t time, zero at impact

p operator $\frac{\partial}{\partial t}$

n integers 1, 2, 3, etc., designating a particular mode of vibration

θ_n nth positive root of equation $1 + \cos\theta \cosh\theta + r\theta(\sinh\theta \cos\theta - \cosh\theta \sin\theta) = 0$

r ratio of tip mass to beam mass $\frac{M}{m}$

ω_n undamped natural angular frequency of nth mode, radians per second $\left(\rho c \frac{\theta_n^2}{L^2}\right)$

ω_n' damped natural angular frequency of nth mode, radians per second $\left(\omega_n \sqrt{1 - \frac{\lambda^2 \omega_n^2}{4E^2}}\right)$

$\left(\text{where } \frac{\lambda^2 \omega_n^2}{4E^2} > 1, \text{ the "frequency" is defined by } \omega_n' = \omega_n \sqrt{\frac{\lambda^2 \omega_n^2}{4E^2} - 1}\right)$

v velocity of beam prior to impact

$w(x,t)$ deflection of beam at station x and time t

$w_n(x,t)$ deflection of beam at station x and time t for the nth mode of vibration

$a(x,t)$ acceleration of beam at station x and time t

$a_n(x,t)$ acceleration of beam at station x and time t for nth mode of vibration

$\sigma(x,y,t)$ bending stress in beam at station x, distance from neutral axis y, and time t

$\sigma_n(x,y,t)$ bending stress in beam at station x, distance from neutral axis y, and time t for nth mode of vibration

$\bar{\tau}(x,t)$ average shear stress over cross section of beam at station x and time t

$\bar{\tau}_n(x,t)$ average shear stress over cross section of beam at station x and time t for nth mode of vibration

A_n bending-stress coefficient for nth mode of vibration

B_n shear-stress coefficient for nth mode of vibration

C_n deflection coefficient for nth mode of vibration

RESULTS AND CONCLUSIONS

Theoretical

When a cantilever beam with a mass at its tip is under uniform translation in a direction perpendicular to its length there is excited a theoretically infinite number of modes of vibration when its root is instantaneously brought to rest. With each successive mode, damping has an increasing influence upon the frequencies and amplitudes of vibration and, for sufficiently high modes, even changes the type of motion from oscillatory to nonoscillatory motion. In the lower modes, however, damping has little effect and only terms of the first order in damping need be included in the equations. Only the equations applicable

to the lower modes, which alone are of importance in any practical case, are presented in this section of the paper. For a more complete treatment of damping, see appendix A.

The angular frequencies (2π times the frequencies in cps) are given by the equation

$$\omega_n = \rho c \frac{\theta_n^2}{L^2} \tag{1}$$

where θ_n is the nth positive root of the equation

$$1 + \cos\theta \cosh\theta + r\theta(\sinh\theta \cos\theta - \cosh\theta \sin\theta) = 0 \tag{2}$$

In this equation r is the ratio of the tip mass to the mass of the beam. The values of θ_n for the first three modes are given in the following table for several values of r:

r	θ_1	θ_2	θ_3
0	1.8751	4.6941	7.8548
$\frac{1}{4}$	1.5738	4.2250	7.2813
$\frac{1}{2}$	1.4200	4.1105	7.1904
$\frac{3}{4}$	1.3202	4.0602	7.1539
1	1.2479	4.0311	7.1339
2	1.0774	3.9826	7.1026
4	.9174	3.9557	7.0859
6	.8328	3.9460	7.0802

Figure 1 shows graphically the variation of θ_n with the mass ratio r for $n = 1$, 2, and 3. For each value of n the value of θ_n, and consequently the frequency, decreases with increasing values of the mass ratio r.

Expressions for the bending stresses, shear stresses, deflections, and accelerations are the same as the expressions given in reference 1 for these quantities except that the coefficients A_n, B_n, and C_n, which characterize each mode, are functions of an additional variable r, the mass ratio. The bending stress, average shear stress, and deflection are, respectively, for the nth mode of vibration:

$$\sigma_n(x,y,t) = A_n \frac{v}{c} \frac{y}{\rho} E e^{-\frac{\lambda \omega_n^2}{2E} t} \sin \omega_n t \tag{3}$$

$$\bar{\tau}_n(x,t) = B_n \frac{v}{c} \frac{\rho}{L} E e^{-\frac{\lambda \omega_n^2}{2E} t} \sin \omega_n t \tag{4}$$

$$w_n(x,t) = C_n \frac{v}{c} \frac{L^2}{\rho} e^{-\frac{\lambda \omega_n^2}{2E} t} \sin \omega_n t \tag{5}$$

The acceleration for the nth mode, when damping is sufficiently small, is

$$a_n(x,t) = -\omega_n^2 w_n(x,t) \tag{6}$$

The variation of the dimensionless coefficients A_n, B_n, and C_n with position along the beam x/L is given in figures 2, 3, and 4, respectively, for the first three modes, $n = 1$, 2, and 3 and for values of r from 0 to 6. Figures 2 and 3 indicate that for all values of the mass ratio r the highest values of A_n and B_n and hence the highest stresses occur at the root of the beam. These highest or root values of A_n and B_n are shown for $r = 0$ and $r = 6$ in figure 5 for the first 5 modes. Root values of A_n and B_n for mass ratios between 0 and 6 are given in figure 6 for the first 3 modes. Both figures 5 and 6 show that the addition of a mass at the tip of the beam ($r > 0$) increases appreciably the values of the stress

coefficients A_n and B_n for the first mode ($n = 1$) but has a very small effect upon these coefficients for the second and higher modes.

The tip mass increases the maximum bending stress much less than might be expected on the basis of static considerations. For example the addition of a tip mass 6 times the mass of the beam increases the mass moment about the root 1200 percent whereas the first mode bending stress coefficient A_1 is increased only 184 percent (from 1.566 to 4.450). (See fig. 5.)

The maximum values with respect to time of $\sigma_n(x,y,t)$ and $\bar{\tau}_n(x,t)$ associated with the nth mode of vibration, when the effects of damping are neglected, are

$$\sigma_n(x,y) = A_n \frac{v}{c} \frac{y}{\rho} E \tag{7}$$

$$\bar{\tau}_n(x) = B_n \frac{v}{c} \frac{\rho}{L} E \tag{8}$$

Equations (3) and (4) for bending and shear stress, from which equations (7) and (8) are obtained, and equations (5) and (6) for deflections and accelerations give the values associated with the nth mode of vibration. Since all modes of vibration occur simultaneously the net results are the superposition of the effects of all modes. This superposition gives the following equations:

$$\sigma(x,y,t) = \frac{v}{c} \frac{y}{\rho} E \left(A_1 e^{-\frac{\lambda\omega_1^2}{2E} t} \sin \omega_1 t + A_2 e^{-\frac{\lambda\omega_2^2}{2E} t} \sin \omega_2 t + \ldots \right) \tag{9}$$

For average shear stress,

$$\bar{\tau}(x,t) = \frac{v}{c}\frac{\rho}{L}E\left(B_1 e^{-\frac{\lambda\omega_1^2}{2E}t}\sin\omega_1 t + B_2 e^{-\frac{\lambda\omega_1^2}{2E}t}\sin\omega_2 t + \ldots\right) \tag{10}$$

For deflection,

$$w(x,t) = \frac{v}{c}\frac{L^2}{\rho}\left(C_1 e^{-\frac{\lambda\omega_1^2}{2E}t}\sin\omega_1 t + C_2 e^{-\frac{\lambda\omega_2^2}{2E}t}\sin\omega_2 t + \ldots\right) \tag{11}$$

For acceleration, when damping is sufficiently small,

$$a(x,t) = -\frac{v}{c}\frac{L^2}{\rho}\left(C_1\omega_1^2 e^{-\frac{\lambda\omega_1^2}{2E}t}\sin\omega_1 t + C_2\omega_2^2 e^{-\frac{\lambda\omega_2^2}{2E}t}\sin\omega_2 t + \ldots\right) \tag{12}$$

For a beam with a given cross section and velocity at impact, the equations for bending stress reveal that at a given percentage of the distance from root to tip and for a given mass ratio, the bending stress for a particular mode is independent of the length of the beam. The equations for shear stress reveal that the shear stress at any station varies inversely with the length of the beam.

Experimental

The apparatus which was used to provide for the instantaneous arrest of a cantilever beam is shown in figure 7. In this apparatus two cantilever beams are formed by centrally clamping a steel tube in a heavy split block. The block is attached to a carriage which is permitted to run with known velocity over a horizontal track. The carriage is accelerated by a weight acted upon by gravity in the initial portion of the run and is kept in a state of uniform translation by an additional small weight used to overcome friction in the latter portion of the run. Instantaneous arrest is achieved by permitting a tapered plug projecting from the carriage to ram into a fixed chuck. The effect of a tip mass was studied by increasing the weights on the tips of the beams in successive tests. The velocity at impact and the dimensions of the cantilever beams are given in appendix B.

The apparatus described herein provides for a much more rigid clamping of the tube and gives a better control over the instantaneous arrest than the apparatus described in reference 1. With the more rigid clamping, less oscillatory energy was lost by the cantilever beams to adjacent parts of the apparatus. The damping present, therefore, more nearly approached the damping of the material of the beam.

Extreme fiber bending stresses near the root of each cantilever beam were measured by means of electrical strain gages and a recording oscillograph as described in reference 1. A typical record of the bending strains at the roots of the two cantilever beams with the mass ratio $r = \frac{1}{4}$ is shown in figure 8. No measurements were made of the shear stresses since their values were too small to be measured accurately in the presence of the vibrations set up by the rolling of the carriage.

The three quantities that were obtained from the tests - the frequencies of the first three modes, the maximum contribution of the first mode to the total extreme fiber bending stress at the root, and the maximum extreme fiber bending stress at the root - are plotted against the mass ratio r in figures 9 and 10 for comparison with the theoretically computed values. Since inherent local variations in the beam

properties do not appreciably affect the frequencies, which are associated with the over-all action of the beam, and since frequencies are easy to measure, it is reasonable to expect the observed good agreement between theoretical and experimental frequencies. (See fig. 9.) When consideration is given to the fact that stresses are directly affected by the local variations in the beam properties and are not readily susceptible to instantaneous accurate measurement the observed agreement between the experimental and theoretical stresses is also considered to be satisfactory. (See fig. 10.)

The contribution of the first mode to the total stress was estimated from the records. (See fig. 8.) It is clear from figure 10 that the first mode contributes more than half of the total stress. It is also clear from figure 10 that for practical engineering analysis the maximum bending stress developed in a suddenly arrested cantilever beam can be found by a simple addition of stress amplitudes in the first few modes (in this case 3) without regard to phase relations between the modes.

Langley Memorial Aeronautical Laboratory
National Advisory Committee for Aeronautics
Langley Field, Va., November 30, 1944

APPENDIX A

THEORETICAL DERIVATION

General analysis.- Consider in equilibrium a uniform cantilever beam with a mass at its free end. If the root of the beam is suddenly disturbed, as by a shock, in a direction perpendicular to its length, the beam will be set into damped bending oscillations. The equation of motion for these bending oscillations is given by the differential equation (reference 1)

$$E\rho^2 \frac{\partial^4 w}{\partial x^4} + \lambda\rho^2 \frac{\partial^5 w}{\partial x^4 \partial t} + \frac{\gamma}{g}\frac{\partial^2 w}{\partial t^2} = 0 \qquad \text{(A1)}$$

With the use of the notation $c^2 = \frac{gE}{\gamma}$ equation (A1) may be written

$$\frac{\partial^4 w}{\partial x^4} + \frac{\lambda}{E}\frac{\partial^5 w}{\partial x^4 \partial t} + \frac{1}{\rho^2 c^2}\frac{\partial^2 w}{\partial t^2} = 0 \qquad \text{(A2)}$$

This partial differential equation is reduced to an ordinary differential equation of the 4th order by writing $p \equiv \frac{\partial}{\partial t}$; thus,

$$\left(1 + \frac{\lambda p}{E}\right)\frac{d^4 w}{dx^4} + \frac{p^2}{\rho^2 c^2} w = 0 \qquad \text{(A3)}$$

The general solution of equation (A3) is

$$w = P \cosh \theta\frac{x}{L} + Q \sinh \theta\frac{x}{L} + R \cos \theta\frac{x}{L} + S \sin \theta\frac{x}{L} \qquad \text{(A4)}$$

where

$$\theta = L\sqrt{\frac{ip}{\rho c\sqrt{1+p\frac{\lambda}{E}}}}$$

The coefficients P, Q, R, and S are to be determined from the boundary conditions. The case under consideration is that of a cantilever with a mass at its free end moving with uniform velocity v and having its root brought instantaneously to rest. The boundary conditions for this case are

$$\left(\frac{\partial w}{\partial t}\right)_{x=0} \equiv p(w)_{x=0} = v - v\mathit{1}$$

$$\left(\frac{\partial w}{\partial x}\right)_{x=0} = \left(\frac{\partial^2 w}{\partial x^2}\right)_{x=L} = 0$$

$$EI\left(\frac{\partial^3 w}{\partial x^3}\right)_{x=L} = \frac{M}{g}\left(\frac{\partial^2 w}{\partial t^2}\right)_{x=L} = \frac{M}{g}\,p^2(w)_{x=L}$$

The fourth boundary condition, which is an application of Newton's third law, equates the shear force at the tip of the beam to the inertia force of the tip mass. The velocity of the root as given by the first boundary condition is represented graphically in figure 11. Following the procedure adopted in reference 1, the solution will be obtained for the boundary condition

$$\left(\frac{\partial w}{\partial t}\right)_{x=0} \equiv p(w)_{x=0} = -v\mathit{1}$$

and to the resulting velocity will be added the constant velocity v.

With the application of the boundary conditions to equation (A4), the operational solution for the velocity (that induced by $-v\mathit{1}$) is found to be

$$pw = \frac{-v\mathit{1}}{2} \frac{f\left(\theta\frac{x}{L}\right)}{1 + \cos\theta\cosh\theta + r\theta(\sinh\theta\cos\theta - \cosh\theta\sin\theta)} \tag{A5}$$

where

$$\begin{aligned} f\left(\theta\frac{x}{L}\right) = {} & (1 + \cos\theta\cosh\theta)\left(\cosh\theta\frac{x}{L} + \cos\theta\frac{x}{L}\right) \\ & + \sin\theta\sinh\theta\left(\cosh\theta\frac{x}{L} - \cos\theta\frac{x}{L}\right) \\ & + (\sinh\theta\cos\theta + \cosh\theta\sin\theta)\left(\sin\theta\frac{x}{L} - \sinh\theta\frac{x}{L}\right) \\ & + 2r\theta\left[\sinh\theta\cos\theta\cosh\theta\frac{x}{L} - \cosh\theta\sin\theta\cos\theta\frac{x}{L}\right. \\ & \left. + \cos\theta\cosh\theta\left(\sin\theta\frac{x}{L} - \sinh\theta\frac{x}{L}\right)\right] \end{aligned}$$

and r is the ratio $\frac{M}{m} = \frac{\text{Tip mass}}{\text{Beam mass}}$. Interpretation of this operational expression and addition of the constant velocity v gives for the total velocity

$$\frac{\partial w(x,t)}{\partial t} = v - v\mathit{1} + 2v\sum_{n-1}^{\infty} F\left(\theta_n\frac{x}{L}\right)e^{-\frac{\lambda\omega_n^2}{2E}t}\left(\cos\omega_n' t - \frac{\frac{\lambda\omega_n}{2E}}{\sqrt{1 - \frac{\lambda^2\omega_n^2}{4E^2}}}\sin\omega_n' t\right)\mathit{1} \tag{A6}$$

where

θ_n nth positive root of the frequency equation
$1 + \cos\theta \cosh\theta + r\theta(\sinh\theta \cos\theta - \cosh\theta \sin\theta) = 0$
(all roots, namely $\pm\theta_n$, $\pm i\theta_n$, have been considered in the interpretation)

$\omega_n = pc \dfrac{\theta_n^2}{L^2}$ undamped natural frequency of nth mode, radians/sec

$\omega_n' = \omega_n \sqrt{1 - \dfrac{\lambda^2 \omega_n^2}{4E^2}}$ damped natural angular frequency of nth mode, radians/sec

$$F\left(\theta_n \frac{x}{L}\right) = \frac{\left\{\begin{array}{l} (1 + \cos\theta_n \cosh\theta_n)\left(\cosh\theta_n \frac{x}{L} + \cos\theta_n \frac{x}{L}\right) \\ + \sin\theta_n \sinh\theta_n\left(\cosh\theta_n \frac{x}{L} - \cos\theta_n \frac{x}{L}\right) \\ + (\sinh\theta_n \cos\theta_n + \cosh\theta_n \sin\theta_n)\left(\sin\theta_n \frac{x}{L} - \sinh\theta_n \frac{x}{L}\right) \\ + 2r\theta_n\left[\sinh\theta_n \cos\theta_n \cosh\theta_n \frac{x}{L} - \cosh\theta_n \sin\theta_n \cos\theta_n \frac{x}{L}\right. \\ \left. + \cos\theta_n \cosh\theta_n\left(\sin\theta_n \frac{x}{L} - \sinh\theta_n \frac{x}{L}\right)\right] \end{array}\right\}}{\theta_n\left[(1+r)(\sinh\theta_n \cos\theta_n - \cosh\theta_n \sin\theta_n) - 2r\theta_n \sinh\theta_n \sin\theta_n\right]}$$

Integration of equation (A6) with respect to time with the condition $(w)_{t=0} = 0$ gives for the deflection when $t \geq 0$

$$w(x,t) = 2v\sum_{n=1}^{\infty} \frac{F\left(\theta_n \frac{x}{L}\right)}{\omega_n'} e^{-\frac{\lambda\omega_n^2}{2E}t} \sin \omega_n' t$$

$$= \frac{v}{c}\frac{L^2}{\rho}\sum_{n=1}^{\infty} C_n \frac{1}{\sqrt{1 - \dfrac{\lambda^2\omega_n^2}{4E^2}}} e^{-\frac{\lambda\omega_n^2}{2E}t} \sin \omega_n' t \quad \text{(A7)}$$

where

$$C_n = \frac{2F\left(\theta_n \frac{x}{L}\right)}{\theta_n^{\,2}}$$

The contribution of the nth mode to the deflection is

$$w_n(x,t) = \frac{v}{c}\,\frac{L^2}{\rho}\,C_n\,\frac{1}{\sqrt{1 - \frac{\lambda^2\omega_n^{\,2}}{4E^2}}}\,e^{-\frac{\lambda\omega_n^{\,2}}{2E}t}\,\sin\omega_n'\,t \qquad \text{(A8)}$$

When $\frac{\lambda\omega_n}{2E} > 1$ equation (A8) may be put in the form

$$w_n(x,t) = \frac{v}{c}\,\frac{L^2}{\rho}\,C_n\,\frac{1}{\sqrt{\frac{\lambda^2\omega_n^{\,2}}{4E^2} - 1}}\,e^{-\frac{\lambda\omega_n^{\,2}}{2E}t}\,\sinh\omega_n'\,t \qquad \text{(A9)}$$

where now

$$\omega_n' = \omega_n\sqrt{\frac{\lambda^2\omega_n^{\,2}}{4E^2} - 1}$$

The form indicated by equation (A8), where $\frac{\lambda\omega_n}{2E} < 1$, is characteristic of the lower modes and represents damped oscillatory motion. The form indicated by equation (A9), where $\frac{\lambda\omega_n}{2E} > 1$ (damping greater than critical), is characteristic of the higher modes and represents subsidence motion.

From equation (A6) for the velocity and equation (A7) for the deflection, the complete behavior of the cantilever

may be determined. The quantities of interest are the bending stresses, the shear stresses, and to some extent the accelerations. Where damping is present, the equations representing the contribution of the nth mode to these quantities may be given in the two forms indicated by equations (A8) and (A9). In subsequent equations, however, only the form indicated by (A8) is given, because it is characteristic of the modes which are of practical importance.

Bending stresses.- The bending stresses $\sigma(x,y,t)$ at any fiber a distance y from the neutral axis are

$$\sigma(x,y,t) = Ey\frac{\partial^2 w}{\partial x^2} = E\frac{v}{c}\frac{y}{\rho}\sum_{n=1}^{\infty} A_n e^{-\frac{\lambda\omega_n^2}{2E}t}\sin\omega_n' t \,\mathit{1}$$

where

$$A_n = 2\frac{\left\{\begin{array}{l}(1+\cos\theta_n\cosh\theta_n)\left(\cosh\theta_n\frac{x}{L}-\cos\theta_n\frac{x}{L}\right)\\ +\sin\theta_n\sinh\theta_n\left(\cosh\theta_n\frac{x}{L}+\cos\theta_n\frac{x}{L}\right)\\ -(\sinh\theta_n\cos\theta_n+\cosh\theta_n\sin\theta_n)\left(\sinh\theta_n\frac{x}{L}+\sin\theta_n\frac{x}{L}\right)\\ +2r\theta_n\left[\sinh\theta_n\cos\theta_n\cosh\theta_n\frac{x}{L}+\cosh\theta_n\sin\theta_n\cos\theta_n\frac{x}{L}\right.\\ \left.-\cos\theta_n\cosh\theta_n\left(\sinh\theta_n\frac{x}{L}+\sin\theta_n\frac{x}{L}\right)\right]\end{array}\right\}}{\theta_n\left[(1+r)(\sinh\theta_n\cos\theta_n-\cosh\theta_n\sin\theta_n)-2r\theta_n\sin\theta_n\sinh\theta_n\right]}$$

The contribution to bending stress of the nth mode is

$$\sigma_n(x,y,t) = E\frac{v}{c}\frac{y}{\rho}A_n e^{-\frac{\lambda\omega_n^2}{2E}t}\sin\omega_n' t \,\mathit{1}$$

Average shear stresses.- The average shear stress on the cross section is

$$\bar{\tau}(x,t) = E\rho^2 \frac{\partial^3 w}{\partial x^3} = E \frac{v}{c} \frac{\rho}{L} \sum_{n=1}^{\infty} B_n e^{-\frac{\lambda \omega_n^2}{2E} t} \sin \omega_n' t \mathit{1}$$

where

$$B_n = 2 \frac{\left\{\begin{array}{l} (1 + \cos\theta_n \cosh\theta_n)\left(\sinh\theta_n \frac{x}{L} + \sin\theta_n \frac{x}{L}\right) \\ + \sin\theta_n \sinh\theta_n\left(\sinh\theta_n \frac{x}{L} - \sin\theta_n \frac{x}{L}\right) \\ -(\sinh\theta_n \cos\theta_n + \cosh\theta_n \sin\theta_n)\left(\cosh\theta_n \frac{x}{L} + \cos\theta_n \frac{x}{L}\right) \\ + 2r\theta_n\left[\sinh\theta_n \cos\theta_n \sinh\theta_n \frac{x}{L} - \cosh\theta_n \sin\theta_n \sin\theta_n \frac{x}{L}\right. \\ \left. - \cos\theta_n \cosh\theta_n\left(\cosh\theta_n \frac{x}{L} + \cos\theta_n \frac{x}{L}\right)\right] \end{array}\right\}}{(1 + r)(\sinh\theta_n \cos\theta_n - \cosh\theta_n \sin\theta_n) - 2r\theta_n \sin\theta_n \sinh\theta_n}$$

The contribution to average shear stress of the nth mode is

$$\bar{\tau}_n(x,t) = E \frac{v}{c} \frac{\rho}{L} B_n e^{-\frac{\lambda \omega_n^2}{2E} t} \sin \omega_n' t \mathit{1}$$

<u>Accelerations</u>.- From equation (A6), with the aid of the relation

$$pF(t)\mathit{1} = F(0)p\mathit{1} + F'(t)\mathit{1}$$

the acceleration anywhere on the beam is found to be

$$a(x,t) = \frac{\partial^2 w(x,t)}{\partial t^2} = \left[2\sum_{n=1}^{\infty} F\left(\theta_n \frac{x}{L}\right) - 1\right] vp\mathit{1}$$

$$-\frac{v}{c}\frac{L^2}{\rho}\sum_{n=1}^{\infty} C_n \frac{\omega_n^2\left(1-\frac{\lambda^2\omega_n^2}{2E^2}\right)}{\sqrt{1-\frac{\lambda^2\omega_n^2}{4E^2}}} e^{-\frac{\lambda\omega_n^2}{2E}t}\left(\sin\omega_n' t\right.$$

$$\left.+\frac{\frac{\lambda\omega_n}{E}\sqrt{1-\frac{\lambda^2\omega_n^2}{4E^2}}}{1-\frac{\lambda^2\omega_n^2}{2E^2}}\cos\omega_n' t\right)\mathit{1}$$

With the aid of the orthogonal properties of the functions $F\left(\theta_n \frac{x}{L}\right)$ it is possible to show that the quantity

$2\sum_{n=1}^{\infty} F\left(\theta_n \frac{x}{L}\right) - 1$ reduces to zero when $0 < \frac{x}{L} \leq 1$.

At $\frac{x}{L}$ equal to zero the quantity $2\sum_{n=1}^{\infty} F\left(\theta_n \frac{x}{L}\right)$ is zero and only the term $-vp\mathit{1}$ remains. This term indicates that at $t = 0$ there is at the root an infinite acceleration of zero duration.

The contribution to acceleration of the nth mode is

$$a_n(x,t) = -\frac{v}{c}\frac{L^2}{\rho}\omega_n^2 C_n \frac{1-\frac{\lambda^2\omega_n^2}{2E^2}}{\sqrt{1-\frac{\lambda^2\omega_n^2}{4E^2}}} e^{-\frac{\lambda\omega_n^2}{2E}t}\left(\sin\omega_n' t\right.$$

$$\left.+\frac{\frac{\lambda\omega_n}{E}\sqrt{1-\frac{\lambda^2\omega_n^2}{4E^2}}}{1-\frac{\lambda^2\omega_n^2}{2E^2}}\cos\omega_n' t\right)\mathit{1}$$

Comparison with the expression for $w_n(x,t)$ (equation (A8)) shows that the acceleration of each mode is out of phase with the deflection. When damping is sufficiently small, however, the relation between the acceleration and the deflection reduces to the well known result for undamped vibration

$$a_n(x,t) = -\omega_n^2 \, w_n(x,t)$$

APPENDIX B

Numerical Example

Problem.- To calculate the theoretical bending and shear stress at the position of strain gages on the steel tube beam used in the experimental investigation of the present paper for a mass at the tip equal to the mass of the beam, $r = 1$.

Length of beam, L, in.	29.84
Outside diameter of tube, in.	1.003
Distance to extreme fiber, maximum value of y, in.	0.502
Wall thickness of tube, in.	0.029
Radius of gyration of cross section, ρ, in. . . .	0.345
Distance from root of beam to strain gages, x, in.	0.50
Modulus of elasticity, E (assumed), psi	29×10^6
Velocity at impact, v, fps	1.78
Velocity of sound in steel, c, fps	16,600

The effects of damping will be neglected so that equations (7) and (8) may be used. From the foregoing data of this problem

$$\frac{v}{c}\frac{y}{\rho}E = 4500 \text{ psi}$$

$$\frac{v}{c}\frac{\rho}{L}E = 35.8 \text{ psi}$$

The values of A_n and B_n for the different modes are obtained from figures 2 and 3 for $r = 1$ and $\frac{x}{L} = 0.0167$. The computed stresses are given in the following table

Mode, n	A_n	B_n	σ (psi)	$\bar{\tau}$ (psi)
			$(4500 \times A_n)$	$(35.8 \times B_n)$
1	2.18	2.40	9800	86
2	.89	4.1	4010	144
3	.48	4.0	2160	143
Sum of first three stress amplitudes			15,970	373

An approximation of the maximum total stresses can be obtained by adding the stress amplitudes for the first several modes as indicated.

REFERENCE

1. Stowell, Elbridge Z., Schwartz, Edward B., and Houbolt, John C.: Bending and Shear Stresses Developed by the Instantaneous Arrest of the Root of a Moving Cantilever Beam. NACA ARR No. L4I27, 1944.

L-586

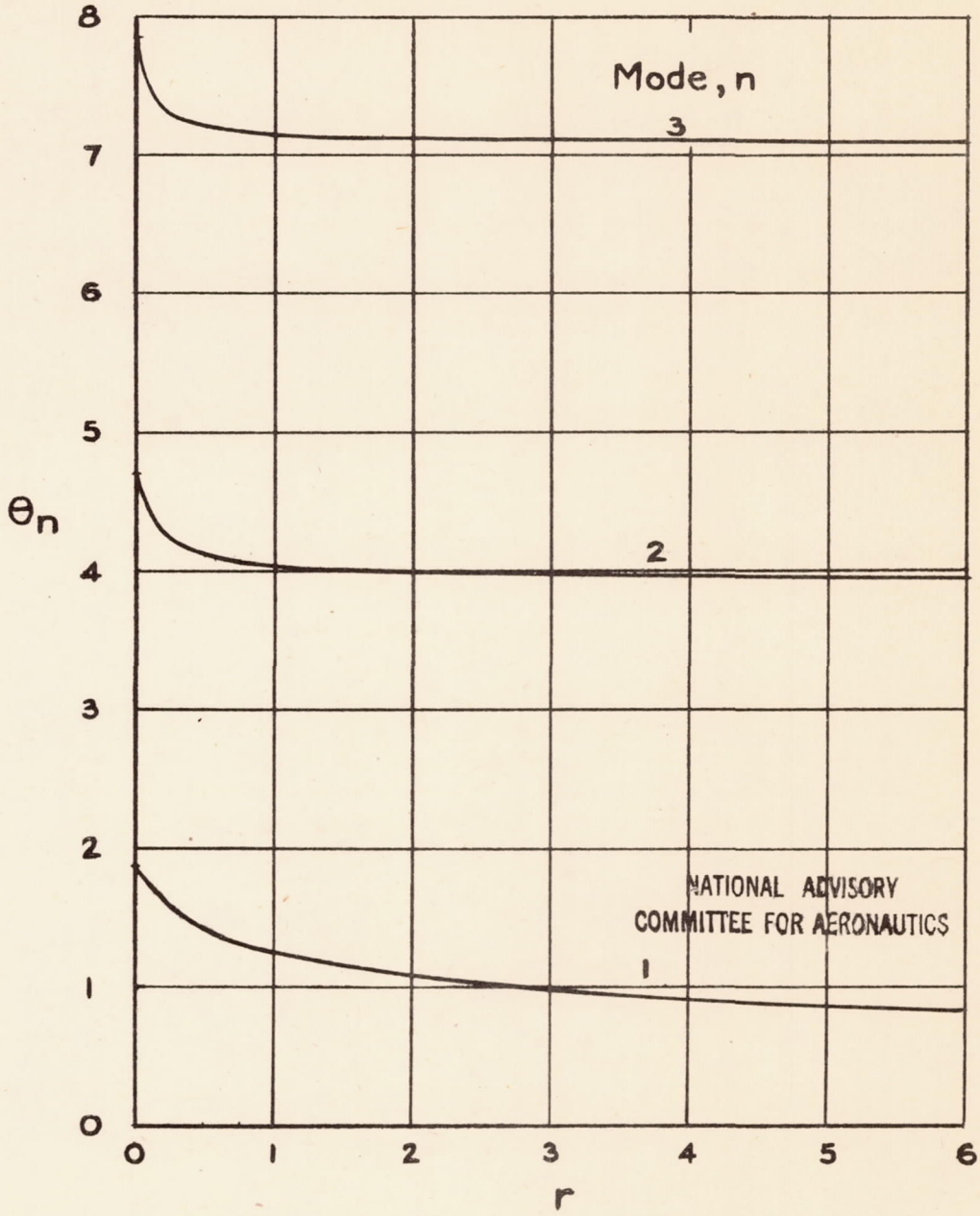

Figure 1.- Variation of θ_n with mass ratio r for n = 1, 2, and 3.

L-586

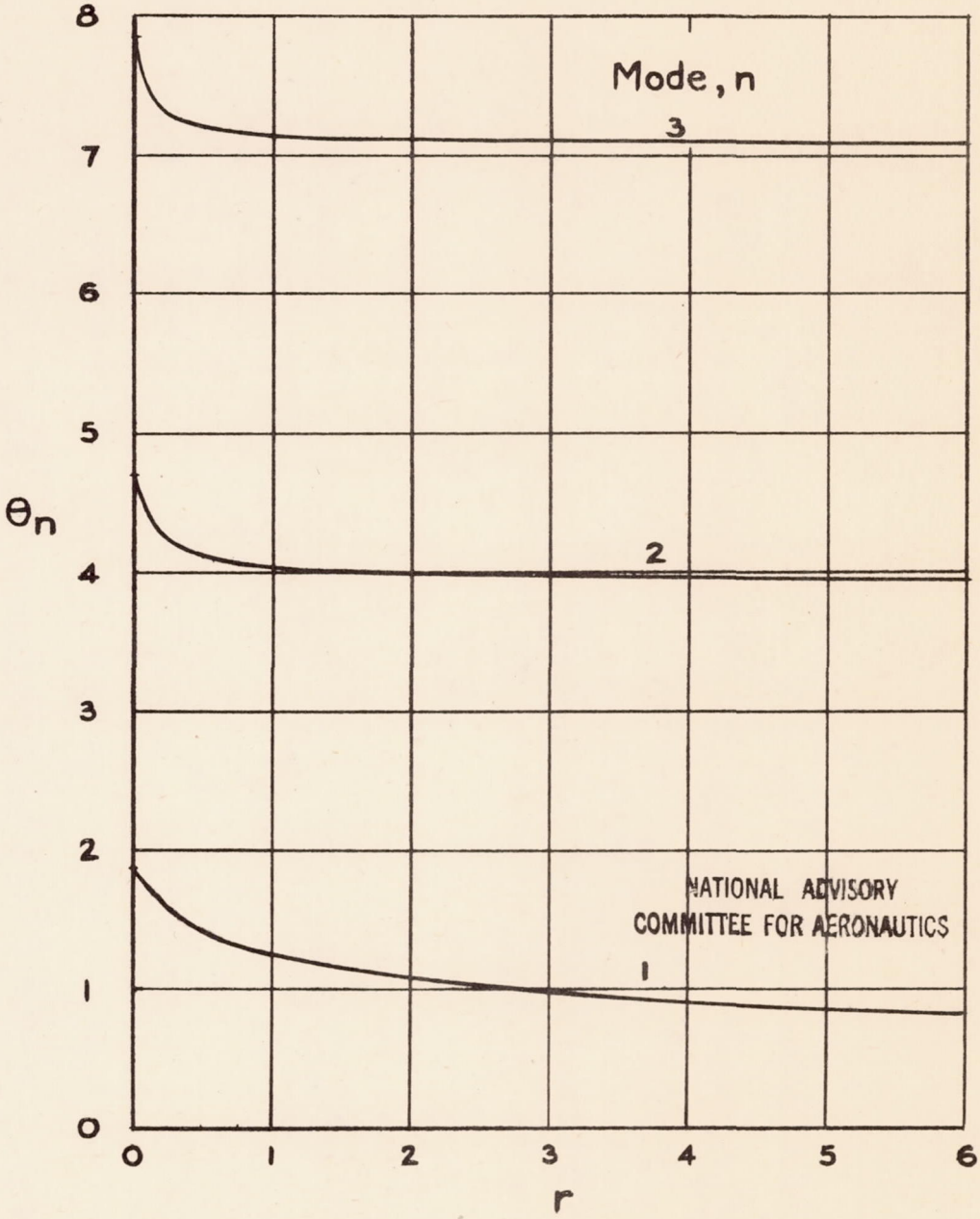

Figure 1.- Variation of θ_n with mass ratio r for n = 1, 2, and 3.

L-586

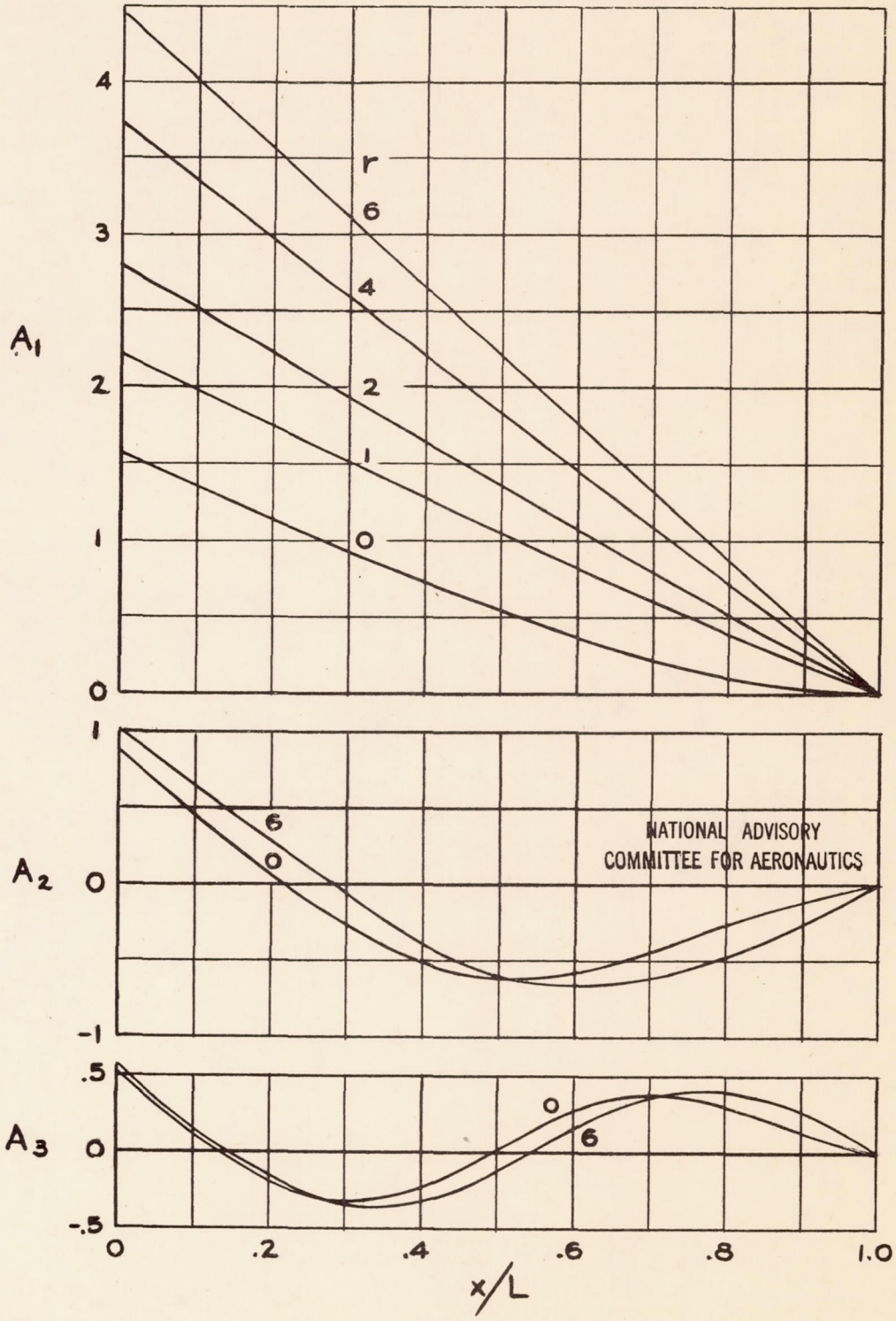

Figure 2.- Variation of bending stress coefficient A_n with x/L.

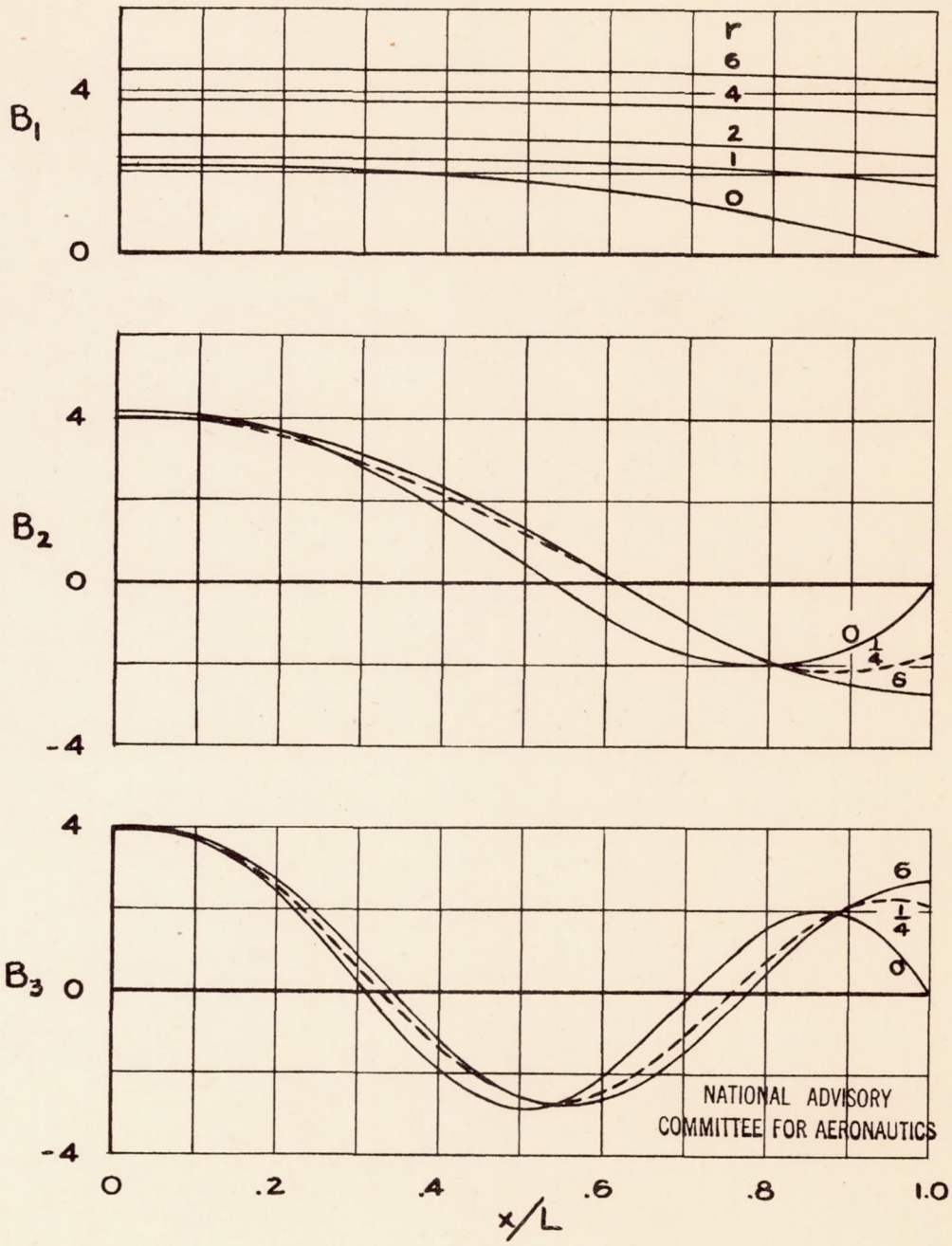

Figure 3. - Variation of shear stress coefficient B_n with x/L.

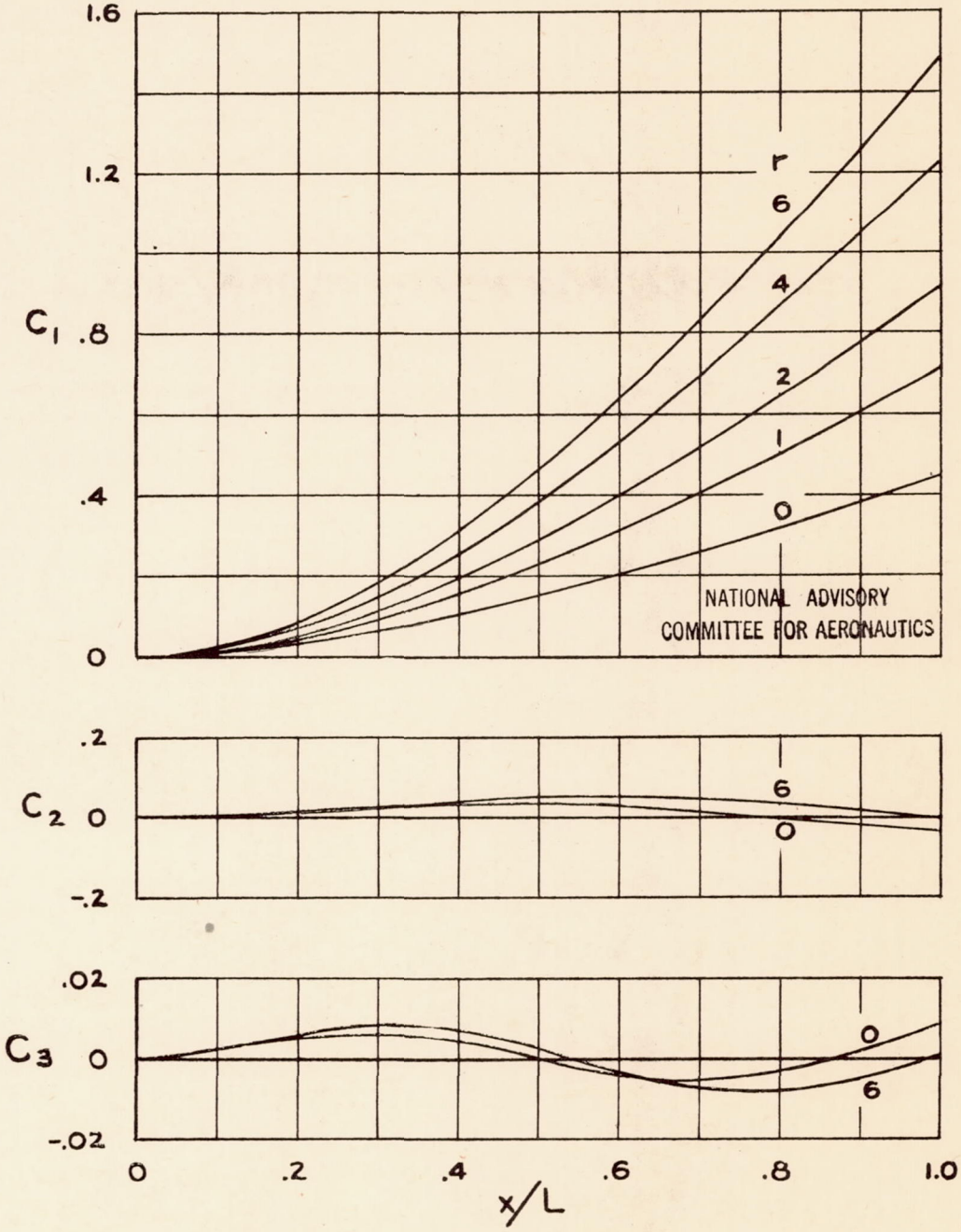

Figure 4.- Variation of deflection coefficient C_n with x/L.

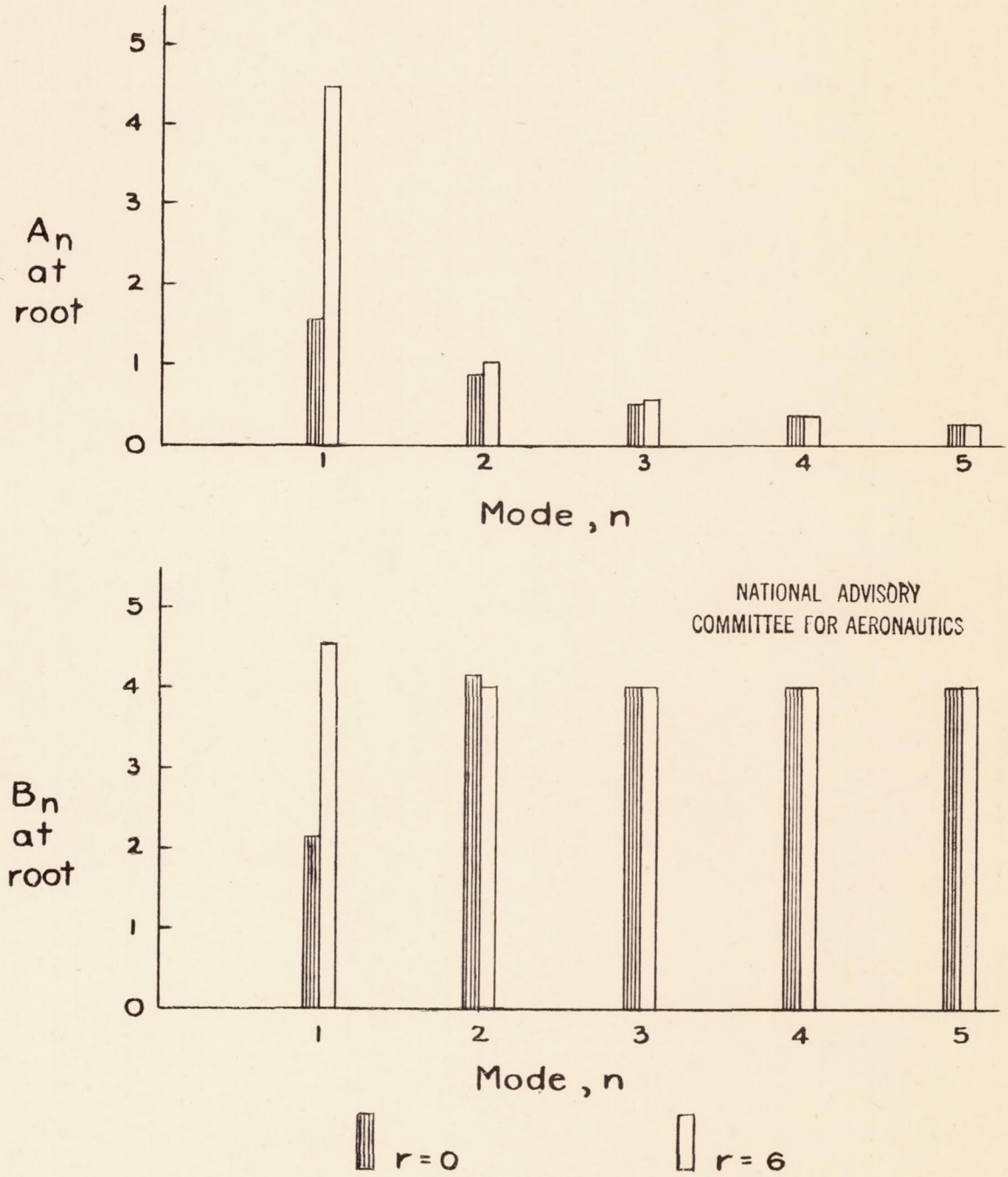

Figure 5.- Values of bending-stress coefficient A_n and shear stress coefficient B_n at root of cantilever beam for mass ratios r = 0 and 6.

L-586

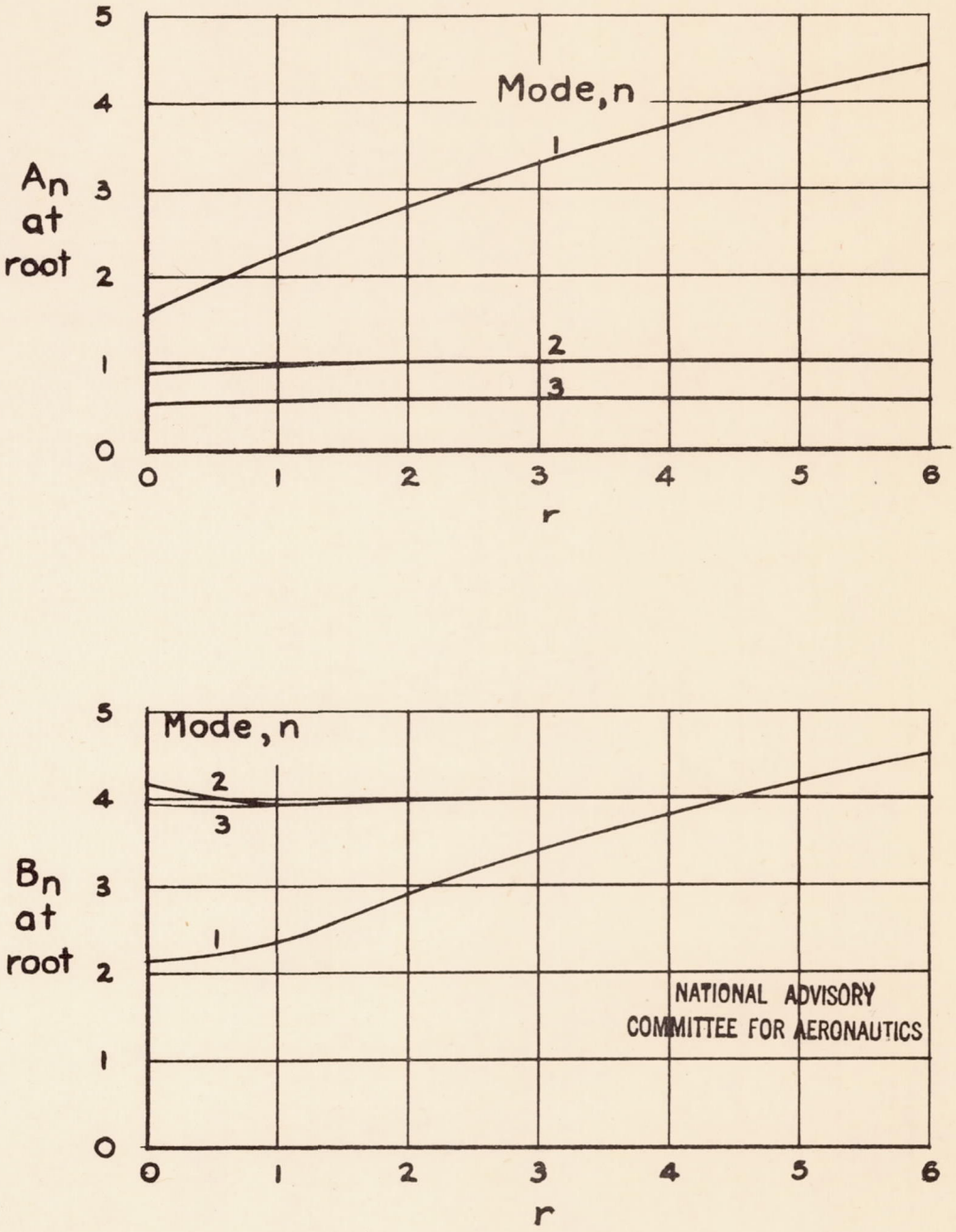

Figure 6.- Variation of bending - stress coefficients A_n and shear-stress coefficients B_n at root of cantilever beam with mass ratio r.

L-586

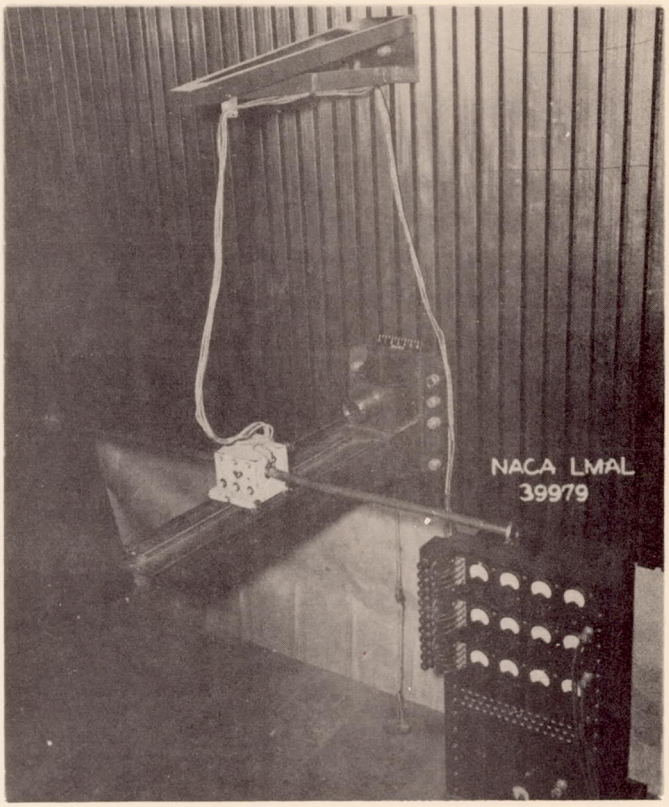

Figure 7.- Impact apparatus used in tests.

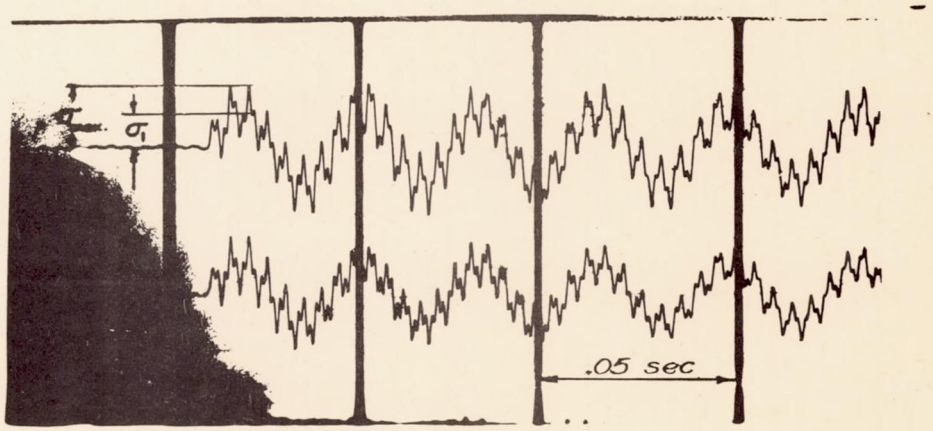

Figure 8.- Typical record of bending strains at the roots of the cantilever beams, mass ratio $r = \frac{1}{4}$.

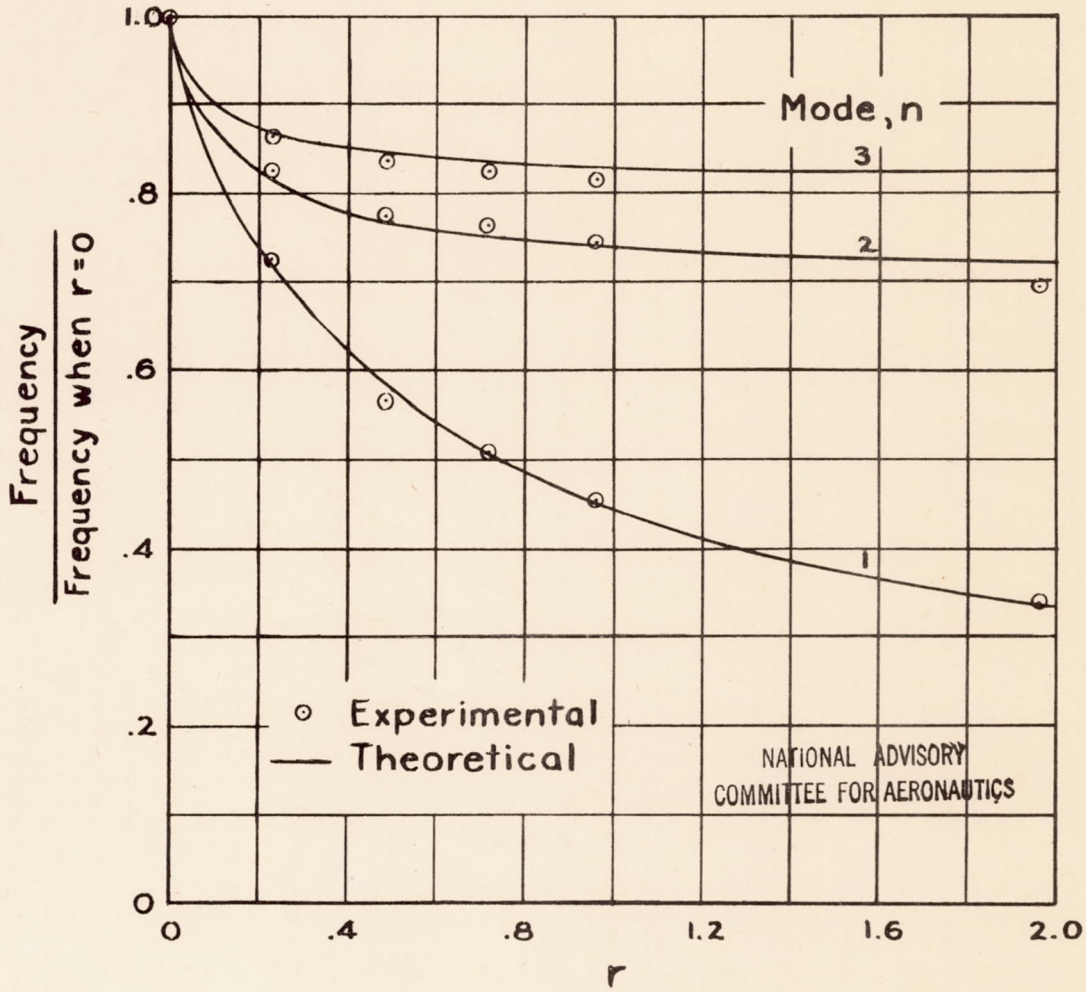

Figure 9.- Comparison of theoretical with experimental frequencies as mass ratio r increases.

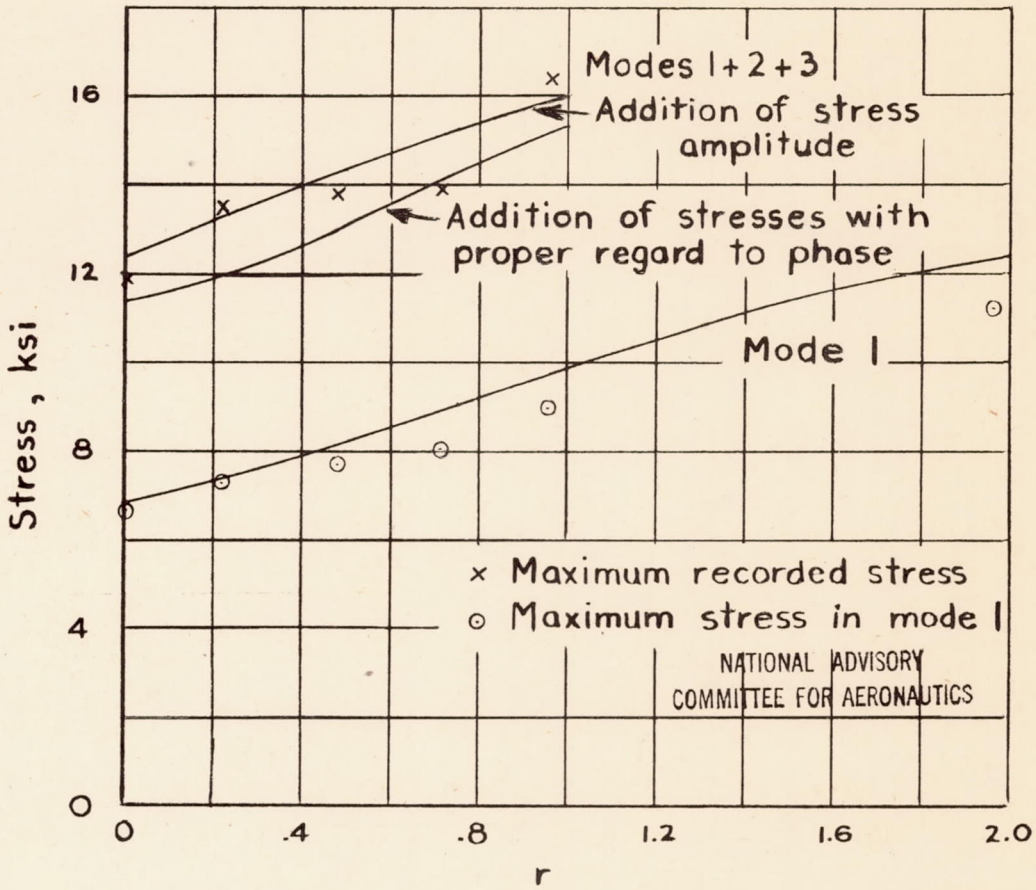

Figure 10. - Comparison of theoretical with experimental root bending stresses as mass ratio r increases.

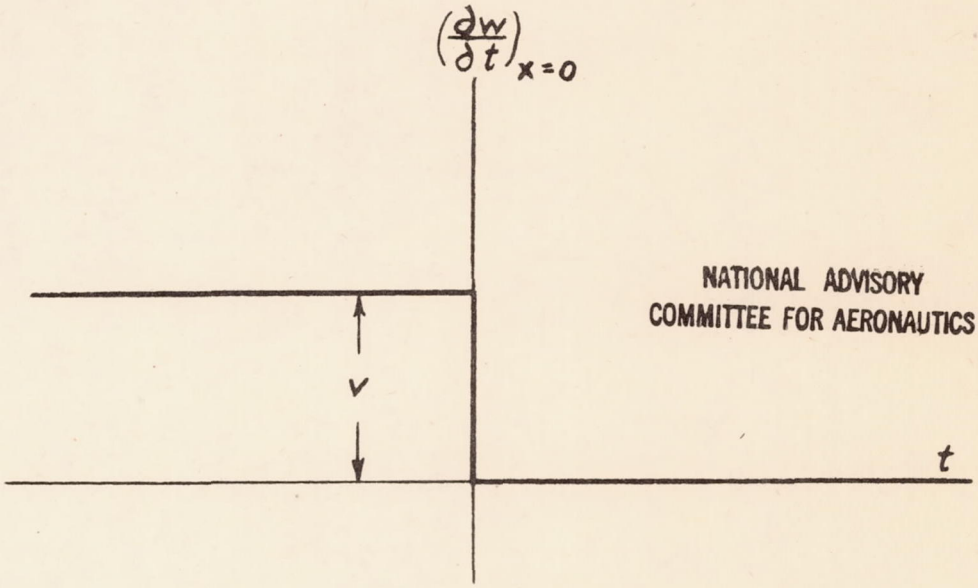

NATIONAL ADVISORY
COMMITTEE FOR AERONAUTICS

Figure 11.- Graphical representation of the discontinuous function v-v1.